DOI 10.5162/iCCC2026/P18

Early Prediction of H_2 Concentration and Sensor Response Using a Multi-Layer Perceptron (MLP)

Raduan Sarif and Carlo Tiebe
Bundesanstalt für Materialforschung und -prüfung (BAM)
Berlin, Germany
Email: raduan.sarif@bam.de; carlo.tiebe@bam.de

Christian Herglotz
Brandenburgische Technische Universität Cottbus-Senftenberg
Cottbus, Germany
Email: christian.herglotz@b-tu.de

Abstract

The hydrogen (H_2) economy is expanding rapidly, promising to be a clean energy solution; however, challenges related to flammability and gas leakage during storage and transportation remain critical. Early monitoring of rising H_2 concentration is crucial for industrial safety and leakage detection; however, in practice, sensor outputs can be subject to drift from the real concentration, resulting in a calibration or adjustment being necessary for an appropriate alarm. To address this limitation, this work presents a Multi-Layer Perceptron (MLP) model that predicts the H_2 concentration and the entire sensor response, including the stable value, using only a 3-second early-time window of the sensor output signal. The proposed approach enables prediction of the final concentration 62% to 92% faster than the traditional t_{90} response time across different H_2 concentration levels. These results demonstrate the potential of fast, model-based prediction to enhance both the speed and reliability of H_2 monitoring systems, thereby supporting the safer deployment of H_2 technologies in real-world applications.

Die Wasserstoffwirtschaft (H_2) gilt als wichtiger Baustein für die Transformation hin zu einer kohlenstofffreien Energieversorgung. Dennoch gibt es Anforderungen für einen sicheren Umgang mit dem Energieträger Wasserstoff zur berücksichtigen. Entlang der Wertschöpfungskette stellen Leckagen ein Sicherheitsdefizit dar. Eine frühzeitige Erkennung ansteigender H_2-Konzentrationen mit Gasdetektoren/Gassensorsystemen, insbesondere in abgeschlossenen Räumen oder zum Freimessen von Komponenten, ist daher von hoher Bedeutung. Diese Arbeit beschreibt die Anwendung des datenanalytischen Modells „Multi-Layer-Perceptron (MLP)“ zur Nutzung eines 3 Sekunden langen Intervalls des Sensorsignals (Zeitreihensignals), um sowohl die H_2-Konzentration als auch den vollständigen Signalverlauf vorherzusagen. Der Ansatz ermöglicht eine Abschätzung der finalen Konzentration um 62% bis 92% schneller als alternative Verfahren zur Beschreibung des transienten Sensorsignalverhaltens. Die Ergebnisse zeigen, dass eine modellbasierte Vorhersage die Geschwindigkeit und Zuverlässigkeit von H_2-Überwachungssystemen erhöht. Die Verwendung dieses Modells in realen Anwendungen trägt somit zur Sicherheit von Wasserstoffgassystemen bei.

1 Introduction

Hydrogen monitoring is essential in storage systems, pipelines, electrolyzers, fuel cells, and refueling stations, where escaping H_2 can accumulate to explosive levels. A reliable monitoring system capable of detecting rising concentrations is therefore critical. Because hydrogen is highly flammable, issuing an alarm before it reaches the ignition threshold—the lower explosion limit (LEL) of 4 Vol% in air [1]—is vital. If the H_2 concentration can be predicted at an early stage, timely safety actions can be initiated. The predicted steady-state sensor response further supports rapid decision-making, thereby reducing the risk of severe incidents.

Recent developments in neural networks have significantly advanced gas sensor technologies, enabling qualitative and quantitative gas identification [2]. In addition to improving accuracy, neural network algorithms have demonstrated the ability to rapidly identify appropriate gases and predict responses by analyzing the transient signals of the sensors [3, 4, 5, 6]. Although these studies show the potential of data-driven approaches, only a few have addressed the prediction of H_2 concentration using a small time window from the early response of the sensor and real H_2 flow, which enables predicting critical H_2 concentrations before they occur [7, 8, 9]. By using the early-time window values of the sensor signal, this study introduces a novel application of the MLP model for three key purposes: (1) predicting the entire sensor response, (2) estimating the stable sensor value, and (3) estimating the real H_2 concentration. This

DOI 10.5162/iCCC2026/P18

concept builds on our previous work [10] [11] [12], using a first-order (FO) exponential model and MLP to predict a stable sensor response from a small time window. This study uses a 3 s early-time window to predict both the sensor response and the H_2 concentration, which falls within the 2 s to 5 s range required for various H_2 safety-critical applications recommended in [13]. Additionally, this work introduces new sensor response datasets, enabling the proposed model to achieve up to 85% faster prediction performance on real sensor time-series data compared to previous methods.

The remaining sections of this paper are structured as follows: Section II describes the data acquisition process; Section III outlines the MLP methodology; Section IV presents the prediction and evaluation results; Section V discusses the model's prediction accuracy; and Section VI concludes the paper.

2 Data Acquisition

For data acquisition in this study, we used the XEN-5320 H_2 thermal conductivity sensor type, whose datasheet specifies a response time of less than 1 s and a t_{90} value of under 5 s [14]. The sensor was mounted on the XEN-85030 gas manifold, which has a volume of (60 mm × 80 mm x 18 mm) and is equipped with standard 5-mm inlet and outlet ports [15]. In accordance with the DIN EN ISO 6145-6 standard [16], H_2 was mixed with air to generate concentrations from 0.1 to 2.0 Vol% at total flow rates of 1000, 1500, 2000, and 3000 mL/min. Each H_2 concentration level duration was maintained for 1 hour, and the sensor's sampling frequency was 1 Hz.

In Fig. 1, each block displays the sensor-measured time series (green) (Vol%) alongside the corresponding H_2 concentration (orange) (Vol%) collected from the mass-flow controller (MFC). In the following figure, the x-axis represents time in hours, while the y-axis shows the sensor response and the corresponding H_2 concentration in Vol%. For total flow rates of 1000, 1500, and 2000 mL/min, 20 experimental time series were recorded. For the 3000 mL/min, only eight time series were obtained due to an MFC malfunction.

Figure 2 presents an example where the given H_2 concentration is 1.0 Vol% at a total flow of 1000 mL/min. In this case, the sensor response (Vol%) (green) reaches approximately 1.45 Vol% for a real concentration of 1.0 Vol% (orange), demonstrating a noticeable bias relative to the actual H_2 level. To address this issue, the proposed MLP model is designed not only to predict the stable sensor response but also to estimate the true underlying H_2 concentration.

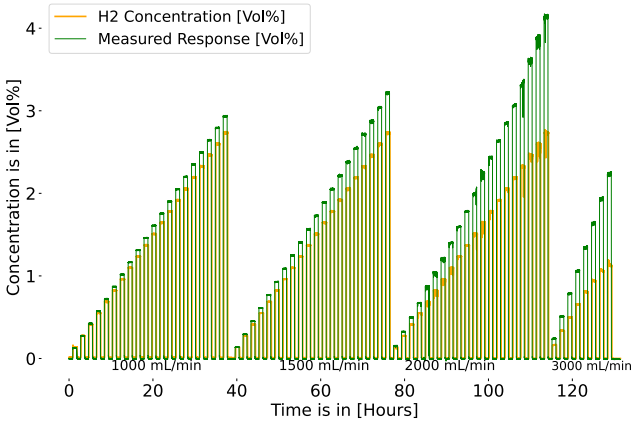

Figure 1: Measured sensor response and corresponding given H_2 concentration (for 0.1 Vol% 2.0 Vol%) at a total flow rate of 1000,1500,2000,3000 mL/min.

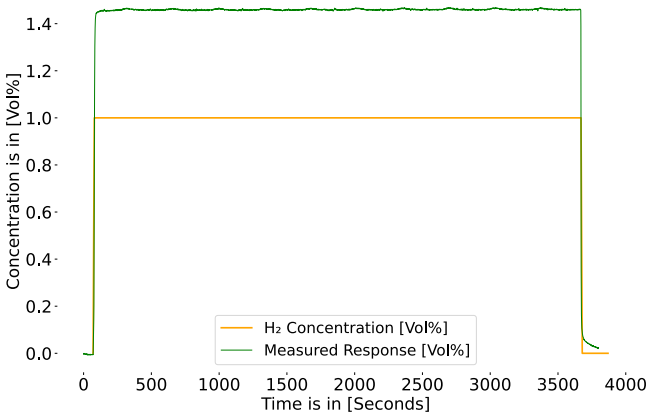

Figure 2: Measured sensor response and corresponding given H_2 concentration (for 1.0 Vol%) at a total flow rate of 1000 mL/min.

3 Methodology of the MLP

In this study, we employ an MLP model [17], whose input layer receives the raw sensor values and forwards them directly to the hidden layers. Each neuron represents one feature of the input data, so the number of input neurons matches the dimensionality of the input vector. The MLP input I_p consists of sensor values extracted from a predefined small-time window, as described in Eq. (1). These input features-i.e., the small time-window samples $S_{\mathrm{w}}(t)$-begin at the time index where the sensor output exceeds the threshold S_{th} and end at the time index t_{w}. The MLP output layer predicts the target quantities defined in Eq. (2), namely sensor time series response up to 600s, the stable sensor value $\hat{S}_{\mathrm{stable}}$ and the corresponding H_2 concentration Y_{H_2}.

$$\boldsymbol{I}_p = [S_w(t_1), S_w(t_2), \ldots, S_w(t_w)] \tag{1}$$

DOI 10.5162/iCCC2026/P18

$$\mathbf{O}_p = \{\hat{S}(t),\ \hat{S}_{\text{stable}},\ Y_{\text{H}}\} \tag{2}$$

In the MLP input and output layers are connected through hidden layers, as illustrated in Fig. 3. Each input to a hidden layer neuron is weighted by a corresponding weight W and added to a bias b. The weights determine the strength of the connections between neurons, while the bias shifts the activation function, allowing the model to adjust the activation threshold. The MLP learns weights and biases during the training process to adaptively fit the training data and capture complex patterns of the datasets.

In Eq. (3), each hidden neuron $h_{j,k}$ computes a weighted sum of the inputs received from the previous layer. Here, k denotes the time index t_w of the input features, and j denotes the index of the neurons in the hidden layer. Here, $I_{p(k)}$ represents the input features at time index k. The resulting weighted sum is then passed through an activation function, typically the Rectified Linear Unit (ReLU), denoted as $f(h_{j,k})$ and defined in Eq. (4). In the subsequent hidden layers, each neuron performs the same computation, but using the outputs of the previous layer instead of the raw sensor inputs. The proposed model uses two hidden layers, each containing $j = 162$ neurons.

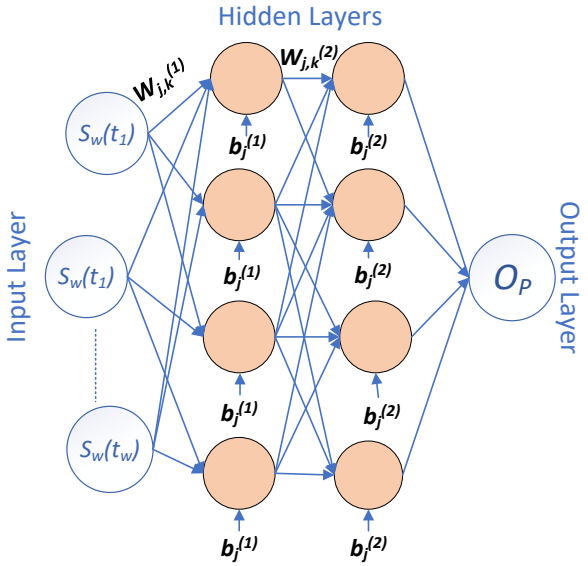

Figure 3: MLP architecture with an input layer, two hidden layers with separate weights for each neuron ($W_{j,k}^{(1)}, W_{j,k}^{(2)}$) and biases ($b_j^{(1)}, b_j^{(2)}$), and an output layer ($O_p$) for stable sensor response prediction [12].

$$h_{j,k} = \sum_{1}^{t_w} I_{p(k)} \cdot W_{j,k} + b_j \tag{3}$$

$$f(h_{j,k}) = \begin{cases} h_{j,k}, & \text{if } h_{j,k} > 0 \\ 0, & \text{if } h_{j,k} \leq 0 \end{cases} \tag{4}$$

Before training the MLP, a Python-based algorithm was developed to automatically detect segments of the sensor time series $S_{\text{r}}(t)$ and the corresponding given H_2 concentration X_{H_2} reported by MFC. The algorithm identifies rising edges where the signals exceed predefined thresholds: $S_{\text{th}} > 0.02$ Vol% for $S_{\text{r}}(t)$ and $X_{H_2}(t) > 0.1$ Vol% for the concentration signal. For each detected segment, a 3600-second sample of both $S_{\text{r}}(t)$ and X_{H_2} is extracted for further processing. These detected segments of $S_{\text{r}}(t)$ and $X_{H_2}(t)$ are then used to construct the training dataset for the MLP. From each segment, the model extracts a short early-time window, the stable sensor value, and the corresponding H_2 concentration.

During testing, the model receives an early-time window from seven randomly selected sensor response time series, representing 10% of the total dataset. This window is scaled and provided as input to generate the predicted sensor response. The predicted curve starts from the last point of the early-time window and extends up to 600 seconds. In the inference stage, the model receives an input vector I_p derived from the early-window features $S_{\text{w}}(t)$ and produces the output vector O_p.

We evaluate the MLP prediction accuracy using the relative fitting error ε defined in Eq. (5), computed between the real sensor response $S_r(t)$ and the model prediction $\hat{S}(t)$. The error is calculated over discrete time indices t_i with a total of N samples. As well as the stable-value prediction error ε_s, shown in Eq. (6) is the relative absolute difference between the true stable value S and its prediction $\hat{S}$, expressed as a percentage.

Similarly, Eq. (7) defines the H_2 concentration prediction error, obtained by comparing the given concentration X_{H_2} with the model-predicted concentration Y_{H_2}. Finally, the relative time savings η_{s} are computed using Eq. (8) by comparing the model's prediction time $\hat{t}$ with the sensor's t_{90} response time. The metric t_{90}, a widely used indicator of sensor response speed [18, 16], was determined in this study through graphical analysis. The total prediction time $\hat{t}$ consists of the early-time window duration t_w plus the MLP inference time. Since the inference time is only a few milliseconds, it was not included in the analysis of this study.

$$\varepsilon = \frac{1}{N} \sum_{i=1}^{N} \left(\frac{|S_r(t_{\text{i}}) - \hat{S}(t_{\text{i}})|}{S_r(t_{\text{i}})} \right) \times 100\% \tag{5}$$

DOI 10.5162/iCCC2026/P18

$$\varepsilon_s = \left| \frac{S - \hat{S}}{S} \right| \times 100\%. \tag{6}$$

$$\varepsilon_{H_2} = \left| \frac{X_{H_2} - Y_{H_2}}{X_{H_2}} \right| \times 100 \tag{7}$$

$$\eta_s = \left(\frac{t_{90} - \hat{t}}{t_{90}} \right) \times 100\% \tag{8}$$

4 Results Analysis

The model validation dataset was generated separately at H_2 concentrations of 0.3, 0.5, 0.7, 1.0, 1.5, and 2.0 Vol% under a total flow rate of 1000 mL/min, using the same experimental procedure. For prediction, the input early-time window $S_w(t)$ consisted of the early 3-second samples above the threshold $S_{\text{th}} > 0.02$ Vol% for each concentration. The MLP predicts the sensor response $\hat{S}(t)$ up to 600 s, including the stable value $\hat{S}$ and the estimated H_2 concentration Y_{H_2}. Figure 4 shows the 1 Vol% result, where the horizontal axis represents time in seconds, and the vertical axis represents the sensor output in Vol%. The blue curve is the 3 s early-time window $S_w(t)$, the green curve is the measured response stable value $S = 1.31$ Vol%, and the red curve is the predicted response $\hat{S}(t)$ (stable value 1.203 Vol%).

The predicted response $\hat{S}(t)$ shows some fluctuations and is slightly lower than the measured stable value. This is expected given the limited size of the training dataset and the simple MLP architecture. Even with these constraints, the model could learn the critical dynamic trend, and the remaining noise and lower estimation can be further improved by training on larger datasets or using a more complex network.

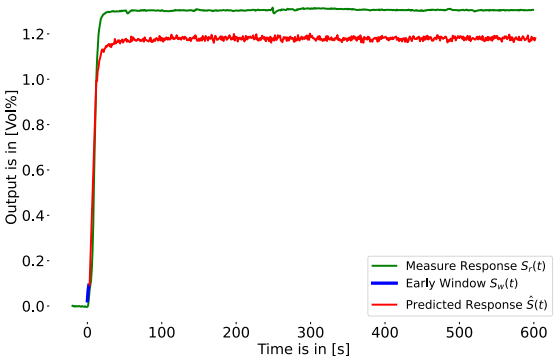

Figure 4: Measured and MLP-predicted sensor response for 1 Vol% H_2 for total flow of 1000 mL/min.

5 Discussion

Table 1 presents the overall MLP validation results for different H_2 concentrations. The real concentration is denoted by X_{H_2} and the predicted concentration by Y_{H_2} (Vol%). Similarly, the real stable sensor output is represented by S and its predicted value by $\hat{S}$ (Vol%), with the corresponding stable-value error ε_s defined in Eq. (6). The H_2 concentration error ε_{H_2} is computed using Eq. (7), and the model relative fitting error ε is calculated using Eq. (5). The relative time savings η_s are determined from Eq. (8), where the prediction time was fixed at $\hat{t} = 3$ s for all H_2 concentrations.

Table 1: Overall MLP Validation Summary for Different H_2 Concentrations

X_{H_2}	Y_{H_2}	ε_{H_2}	S	$\hat{S}$	ε_s	t_{90}	η_s	ε
0.3	0.25	19.00	0.42	0.35	17.27	40	92.68	19.84
0.5	0.49	3.00	0.72	0.58	19.44	31	90.32	15.01
0.7	0.83	18.57	1.01	1.00	1.38	17	82.35	17.14
1.0	1.10	10.30	1.31	1.20	16.18	12	89.00	18.19
1.5	1.60	6.13	2.18	1.94	11.24	10	70.00	17.10
2.0	2.30	18.25	2.92	2.64	9.69	8	62.50	18.09
Mean	–	**12.87**	–	–	**12.53**	–	**81.14**	**17.56**

The MLP time-series prediction demonstrates that the model can learn the rising trend of the H_2 sensor response using only a 3-second early-time window, achieving an accuracy range of 80% to 85% (mean error: 17.56%). The stable-value prediction further demonstrates that the model can reliably estimate the final steady-state level across all validated concentrations, with an accuracy of 83% to 97% (mean error: 12.53%). Overall, the predicted curves follow the general sensor dynamics, reach the stable values, and reproduce the gradual increase toward convergence. In the predicted response curve, some fluctuations are observed, primarily due to the limited size and variability of the real training dataset, as well as the simplicity of the MLP architecture.

In addition, the model also predicts the real H_2 concentration, achieving 80% to 97% accuracy (mean error: 12.87%). Although errors increase at different concentrations due to non-linearities in the MFC values and fewer training samples, the model still reduces the offset between the sensor output and the real H_2 concentration. This ability to estimate the real concentration from only a small early-time window is highly valuable for fast and reliable early-alarming systems. Above all, early-window prediction of the H_2 sensor response can save response time by 62% to 92% (mean time savings 81.14%), enabling much faster H_2 concentration detection compared to the conventional t_{90} time.

6 Conclusion

Overall, the primary objective of this study is to use only the early-time window values of the sensor response to predict the real H_2 concentration, as well as the entire transient sensor response and the final stable value, which are used together as the ground truth for evaluation. By predicting the sensor's entire response before it reaches full convergence, the model can save up to 90% of the time compared to the response time of conventional sensors. This approach enables a fast, reliable, and intelligent H_2 measurement system that enhances industrial safety. It supports future applications such as early leak detection, real-time H_2 concentration monitoring, and a digital twin for hydrogen refueling stations. Since the model estimates the real concentration before the sensor response reaches t_{90}, in any hazardous situation, an alarm system can be triggered earlier and more reliably. In future work, this approach will be validated using a wider range of H_2 concentrations and sensor responses, including the integration of multiple sensors from different sensing principles to improve robustness and generalization.

References

[1] M. Molnarne and V. Schroeder, "Hazardous properties of hydrogen and hydrogen containing fuel gases," *Process Safety and Environmental Protection*, vol. 130, pp. 1–5, 2019.

[2] B. Zong, S. Wu, Y. Yang, Q. Li, T. Tao, and S. Mao, "Smart gas sensors: recent developments and future prospective," *Nano-Micro Letters*, vol. 17, no. 1, p. 54, 2025.

[3] D. L. Osorio-Arrieta, J. L. Muñoz-Mata, G. Beltrán-Pérez, J. Castillo-Mixcóatl, C. O. Mendoza-Barrera, V. Altuzar-Aguilar, and S. Muñoz-Aguirre, "Reduction of the measurement time by the prediction of the steady-state response for quartz crystal microbalance gas sensors," *Sensors*, vol. 18, no. 8, p. 2475, 2018.

[4] R. R. Patil, R. K. Calay, M. Y. Mustafa, and S. Thakur, "Artificial intelligence-driven innovations in hydrogen safety," *Hydrogen*, vol. 5, no. 2, pp. 312–326, 2024.

[5] T. Hübert, J. Majewski, U. Banach, M. Detjens, and C. Tiebe, "Response time measurement of hydrogen sensors," *Hydrogen Knowledge Centre*, 2017.

[6] C. Shi, W. Pei, C. Jin, A. Alizadeh, and A. Ghanbari, "Prediction of the sno2-based sensor response for hydrogen detection by artificial intelligence techniques," *International Journal of Hydrogen Energy*, vol. 48, no. 52, pp. 19834–19845, 2023.

[7] Y. Shi, S. Ye, and Y. Zheng, "Rapid forecasting of hydrogen concentration based on a multilayer cnn-lstm network," *Measurement Science and Technology*, vol. 34, no. 6, p. 065101, 2023.

[8] V. Martvall, H. Klein Moberg, A. Theodoridis, D. Tomecek, P. Ekborg-Tanner, S. Nilsson, G. Volpe, P. Erhart, and C. Langhammer, "Accelerating plasmonic hydrogen sensors for inert gas environments by transformer-based deep learning," *ACS sensors*, 2025.

[9] G. Yang, D. Kong, X. He, X. Yu, and K. Jiang, "Prediction of hydrogen leakage location and intensity in hydrogen refueling stations based on deep learning," *International Journal of Hydrogen Energy*, vol. 68, pp. 209–220, 2024.

[10] R. Sarif, C. Tiebe, and C. Herglotz, "Early response prediction for h2 sensors," in *Proceedings of the 2025 IARIA Annual Congress on Frontiers in Science, Technology, Services, and Applications (IARIA Congress 2025)*, 2025.

[11] R. Sarif, C. Tiebe, and C. Herglotz, "Analysis of methods for predicting h_2 sensor responses," in *Proceedings of the Sensor Measurement Science International (SMSI) Conference*, (Nürnberg, Germany), pp. 169–170, AMA Science, May 2025.

[12] R. Sarif, C. Tiebe, and C. Herglotz, "Early H_2 sensor response prediction using a multi-layer perceptron (mlp)," in *Proceedings of the IEEE Sensors Conference*, (Vancouver, Canada), IEEE, 2025.

[13] T. Hubert, U. Banach, S. Machill, and P. Moretto, "Summary report for a hydrogen sensor workshop," tech. rep., European Commission, Joint Research Centre (JRC), 2017.

[14] Xensor Integration, *XEN-5320-ALU: Thermal Conductivity Gas Sensor*, 2020. Version 30 September 2020.

[15] Xensor Integration, *XEN-85030: Gas Manifold for XEN-5320 Sensor*, 2020. Version 30 September 2020.

[16] International Organization for Standardization, *ISO 26142:2010: Hydrogen detection apparatus – Stationary applications*, 2010. Standard.

[17] L. Piccioni Costa, M. Guerreiro, E. Puchta, Y. Tadano, T. Antonini Alves, M. Kaster, and H. Siqueira, *Multilayer Perceptron*, p. 105. IEEE Computational Intelligence Society Open Book, 01 2023.

DOI 10.5162/iCCC2026/P18

[18] T. Hübert and U. Banach, “Response time of hydrogen sensors,” in *Proceedings of the Fifth International Conference on Hydrogen Safety*, pp. 9–11, 2013.